Physics

Electricity & Magnetism fields

Okayama University *Year* 1999

Thin film write head field analysis using a benchmark problem

Koji Fujiwara* Fumiaki Ikeda† Akihisa Kameari‡
Yasushi Kanai** Kimio Nakamura†† Norio Takahashi‡‡
Koji Tani§ Takashi Yamada¶

*Okayama University
†PHOTON Company Limited, Kyoto
‡Science Solutions International Laboratory, Incorporated
**Niigata Institute of Technology
††Central Research Laboratory, Hitachi, Limited
‡‡Okayama University
§Japan Research Institute, Limited
¶Japan Research Institute, Limited

Thin Film Write Head Field Analysis Using a Benchmark Problem

Koji Fujiwara, Fumiaki Ikeda, Akihisa Kameari, Yasushi Kanai, *Member, IEEE*, Kimio Nakamura, Norio Takahashi, *Fellow, IEEE*, Koji Tani, *Member, IEEE*, and Takashi Yamada, *Member, IEEE*

***Abstract*—A benchmark problem has been proposed by the Storage Research Consortium (SRC) in Japan, for evaluating the applicability of computer codes to 3-D nonlinear eddy current analysis of thin film magnetic recording write head. Various codes using the finite element method are compared in terms of the write head field and the computational efficiency. The difficulty in 3-D mesh generation of thin film head is also discussed. The write head fields calculated by various codes using different meshes show the fairly good agreement. The calculated write head fields are verified by measurement using a stroboscopic electron beam tomography. It is found that the calculation time strongly depends on unknown variables.**

***Index Terms*—Benchmark problem, eddy current, finite element method, thin film write head.**

I. Introduction

THE MAGNETIC recording density increases by the ratio of 60% a year in recent years and the areal density of commercial hard disk drives has reached 10 Gb/in^2. A roadmap shows that hard disk drives with the recording density of 20 Gb/in^2 will be on the market in 2001 and 80 Gb/in^2 in 2005. In order to achieve high transfer rate, recording frequency is expected to be several hundred megahertz. In this situation, large number of reports concerning the spin-valve read heads have been found. On the other hand, write heads have rarely been discussed.

In order to achieve a higher recording density of 20 Gb/in^2 in 2001, SRC was established in 1995 in Japan [1]. The Simulation Working Group for Magnetic Recording in SRC has investigated a benchmark problem for magnetic recording write head analysis to evaluate the applicability of currently proposed numerical methods for magnetic field analysis. In this paper, various 3-D FEM codes using edge elements [2] are applied to the magnetic field analysis of thin film write head of the benchmark problem. The head field is compared at the track center. The difficulty in mesh generation and the behavior of flux density near pole tip of head are discussed.

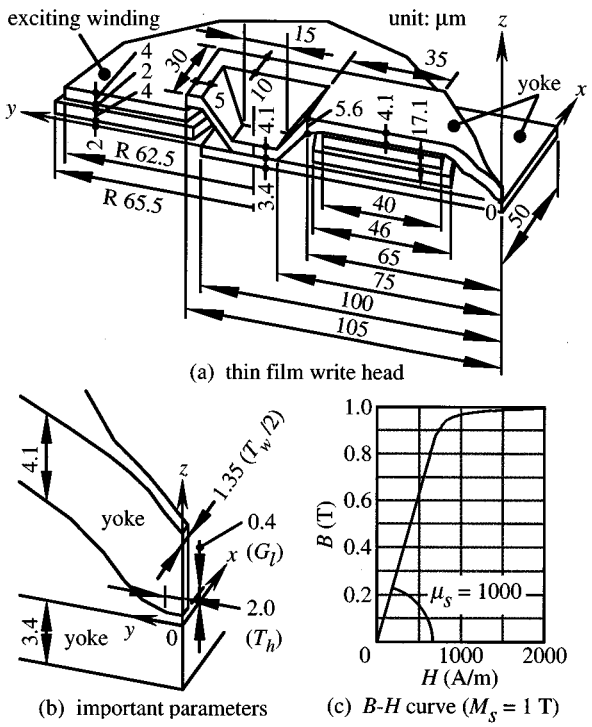

Fig. 1. Benchmark model of thin film write head (2 Gb/in^2).

II. Definition of Benchmark Problem

Fig. 1 shows the benchmark model. The head is used for 2 Gb/in^2 recordings of which the gap length (G_l), throat height (T_h) and track width (T_w) are 0.4 μm, 2.0 μm and 2.7 μm, respectively. The upper and lower yokes are 4.1 μm and 3.4 μm in thickness, respectively. The yoke material is permalloy of which the initial relative permeability μ_s, the saturation magnetization M_s and the conductivity σ are assumed to be 1000, 1 T and 5×10^6 S/m, respectively. The numbers of turns of upper and lower exciting coils are 7 and 8 turns, respectively. The magnetomotive force (*mmf*) shown in Fig. 2 is applied, which is a part of trapezoidal waveform of 25 MHz including higher harmonics. The model is classified as a nonlinear transient eddy

Manuscript received October 25, 1999. This work was supported in part by Storage Research Consortium.

K. Fujiwara and N. Takahashi are with the Department of Electrical and Electronic Engineering, Okayama University, 3-1-1 Tsushima, Okayama 700-8530, Japan (e-mail: {fujiwara, norio}@eplab.elec.okayama-u.ac.jp).

F. Ikeda is with the PHOTON Co., Ltd. 2-1-42 Ayameike-Minami, Nara 631-0033, Japan (e-mail: ikeda@photon-cae.co.jp).

A. Kameari is with the Science Solutions International Laboratory, Inc., 2-21-7 Naka-cho, Meguro-ku, Tokyo 153-0065, Japan (e-mail: kamearia@ssil.com).

Y. Kanai is with the Department of Information and Electoronics Engineering, Niigata Institute of Technology, 1719 Fujihashi, Kashiwazaki 945-1195, Japan (e-mail: kanai@iee.niit.ac.jp).

K. Nakamura is with the Central Research Laboratory, Hitachi, Ltd., 1-280 Koigakubu, Kokubunji, Tokyo 185-8601, Japan (e-mail: k-nakamu@crl.hitachi.co.jp).

K. Tani and T. Yamada are with the Japan Research Institute, Ltd., 16 Ichiban-cho, Chiyoda-ku, Tokyo 102-0082, Japan (e-mail: {tanik@osa; yamada@tyo}.sci.jri.co.jp).

Publisher Item Identifier S 0018-9464(00)06730-3.

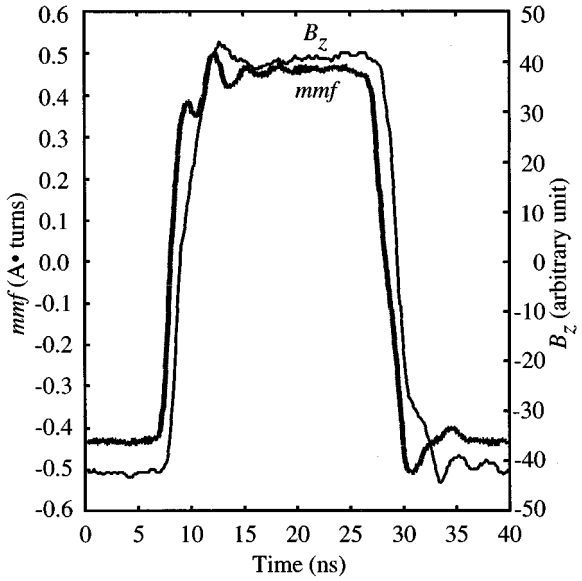

Fig. 2. Applied magnetomotive force and integration of flux density along electron orbit (measured).

current model. The detailed dimensions of pole tip and the typewritten data of applied *mmf* is described in the appendix.

The flux density at the track center ($x = 0$ μm, $y = -1.0$ μm, $z = 0.2$ μm) should be examined. The flux densities at three points of $z = 13$ μm (bottom surface), 15 μm (near center) and 17.1 μm (top surface) on the center ($x = 0$ μm, $y = 30$ μm) of upper yoke should also be investigated.

III. Methods of Analysis and Measurement

As shown in Table I, eight solutions are given by five groups. Hexahedral or tetrahedral 1st-order edge elements are used. The type of unknown variables, number of elements, etc. are different. The codes of nos. 1, 2, 4 and 5 employ $\boldsymbol{A}$ or $\boldsymbol{A}-\phi$ method [3]. In group no. 3, $\boldsymbol{A}-\phi$ or $\boldsymbol{A}$ method and reduced $\boldsymbol{A}_r$ method are applied in conductive and nonconductive regions, respectively [4].

The magnetic fields near the pole tip are measured by a stroboscopic electron beam tomography [5]. This measurement utilizes a pulsed electron beam which is synchronized with the driving current of the magnetic recording head and which can be fixed on a particular phase of the driving current. The deflection of the pulsed electron beam of a particular phase due to the magnetic field was measured by the position sensor. The time and space resolutions are 0.3 ns and 0.1 μm, respectively. The driving current is measured simultaneously by a current probe having a small impedance. Fig. 2 shows the measured value of the integration of the flux density along the electron orbit and the driving current.

IV. Results and Discussion

A. Computational Efficiency

The CPU time of no. 3.2 is reduced to approximately 70% of that of no. 3.1 on the same workstation in spite of the increase of the number of unknowns. This denotes that the CPU time can be saved by employing the scalar potential ϕ as unknown variable which decreases the number of ICCG iterations [3].

In order to compare the CPU time between different environments, performance is measured using the same ICCG code and linear equations obtained from a linear magnetostatic analysis of this model. The efficiency is calculated using the CPU time, the number of steps of no. 1 and the normalized performance. The efficiency of no. 2 is lower than that of no. 1. The main reason is that a shifted parameter for stabilizing the convergence characteristic of the ICCG procedure [6], [7] is fixed at 2.5. Its optimal value is about 1.2 for this calculation. The other codes determine the optimal value automatically. Compared with nos. 1 and 3.1 which use the same mesh, no. 3.1 has much higher efficiency than no. 1. This is, because the convergence characteristic of the ICCG procedure in no. 3.1 can become a convex one by introducing $\boldsymbol{A}_r$, and the ICCG procedure can be terminated around the minimum residual observed at an early iteration step [8]. Compared with nos. 3.4 and 4 which use tetrahedral elements, the efficiency of no. 3.4 is higher than that of no. 4 for the same reason mentioned above. It seems that a method of varying the convergence criterion for the ICCG procedure with nonlinear iteration steps also affects the efficiency. However, its effect is not clear at present.

B. Mesh Generation

The mesh generation of such a thin head is not easy, because the difference in size between the pole tip (1 μm order) and the whole yoke (100 μm order) is extremely large, and the skin effect is remarkable due to the high frequency. It is required to generate a mesh so that the element size increases gradually from the pole tip to the whole yoke by avoiding the generation of flat elements having high aspect ratio. Then, the following various kinds of mesh generators are applied:

1) *Pile of 2-D Mesh and Modification near the Pole Tip (Hexahedral Element, Nos. 1, 2, 3.1, 3.2)*

   In this technique, firstly, all outlines of model are projected on $x-y$ plane, then 2-D region is subdivided into quadrilateral elements. The 2-D mesh is piled in the z-direction to generate hexahedral elements. The obtained 3-D mesh is modified by tilting the tip of the head. The skin depth is about 1.5 μm under the condition of $\mu_s = 1000$, $\sigma = 5 \times 10^6$ S/m and $f = 25$ MHz (frequency of fundamental harmonic of applied *mmf*). By taking account of the skin depth, the upper and lower yokes are subdivided into five layers.

2) *Combination of Delaunay Tessellation and Octree Technique (Tetrahedral Element, Nos. 4, 5)*

   Firstly, 3-D region to be analyzed is subdivided into tetrahedral elements using Delaunay tessellation. In order to add more nodes, the octree method [9] is applied.

3) *Commercial Mesh Generators Developed for Fluid Analysis and Structural Analysis (Nos. 3.3, 3.4)*

   Meshes composed of hexahedral or tetrahedral elements are generated using commercial software. The desired mesh cannot be obtained directly. Therefore, the

TABLE I
DISCRETIZATION DATA AND COMPUTATIONAL EFFICIENCY

group no.	1	2	3.1	3.2	3.3	3.4	4	5
element shape	hexahedron					tetrahedron		
no. of elements	61,089				100,109	350,265	281,603	
no. of nodes	65,670				105,078	64,629	48,064	
no. of unknowns	174,395			192,319	307,802	430,500	347,422	
no. of non-zeros	2,846,205			3,874,349	5,845,937	4,508,037	2,805,536	
unknowns	A		A-A_r	A-A_r-ϕ			A-ϕ	
CPU time [h] (no. of steps)	73.1 (60)	139.8 (57)	14.6 (56)	9.7 (55)	43.3 (56)	18.3 (55)	67.3 (60)	31.0 (59)
efficiency*1	1	0.70	9.08	13.42	3.06	7.11	2.85	2.97
computer used*2	Alpha 21164A 600MHz	Pentium II 400MHz	SUN ULTRA 1 167MHz				Pentium Pro 200MHz	Alpha 21164A 500MHz
OS	DIGITAL UNIX ver.4.0E	Windows NT ver.4.0	Solaris ver.2.5.1				Windows NT ver.4.0	DIGITAL UNIX ver.4.0B
performance*3 [s] (normalized)	297.5 (1)	419.9 (1/1.41)	577.8 (1/1.94)				780.5 (1/2.62)	380.5 (1/1.27)

*1: efficiency = {(CPU time of no.1) / (no. of steps of no.1)} / {(CPU time) / (no. of steps) * (normalized performance)}
*2: All machine have a single processor.
*3: Performance was measured using the same ICCG code and linear equations.

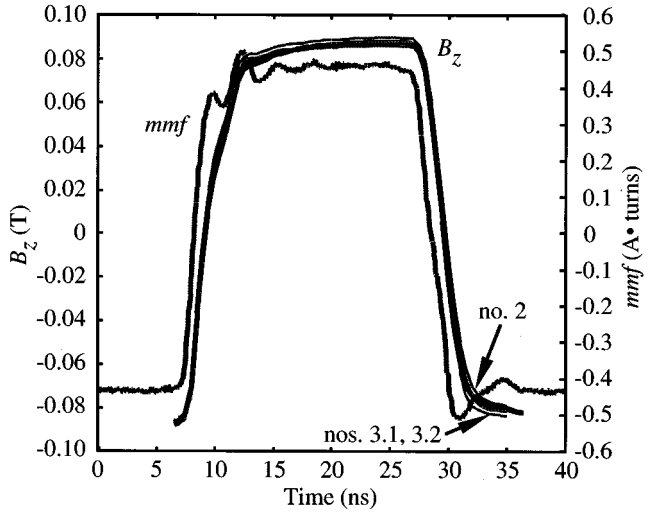

Fig. 3. Time variations of head field.

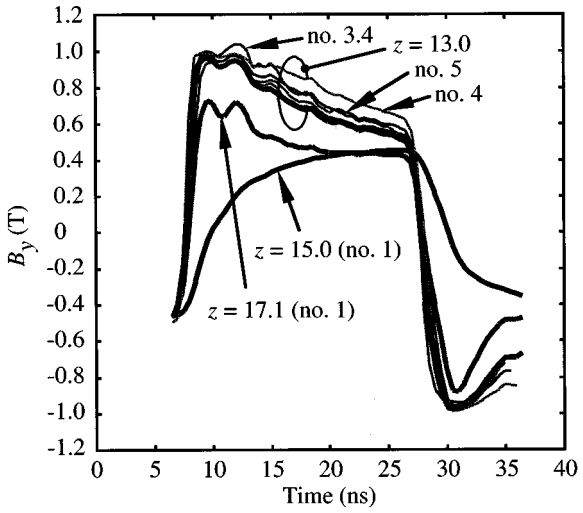

Fig. 4. Time variations of flux density in upper yoke.

improvement may be necessary. The upper and lower yokes are subdivided into ten layers.

The generation of the mesh of such a complicated model is time-consuming. Several days were necessary for generating the mesh including the preparation time of data manually.

C. Head Field and Flux Density in Yoke

Fig. 3 shows the comparison of calculated results of head field B_z at the track center ($x = 0$ μm, $y = -1.0$ μm, $z = 0.2$ μm). Due to the eddy current, the head field is delayed in a few nanoseconds with respect to the applied *mmf*. The head field in high magnetomotive force region is not oscillated due to the saturation of yoke material. The integration of flux density along electron orbit shown in Fig. 2 has the similar tendency as the head field.

Fig. 4 shows the time variation of flux density B_y in the upper yoke ($x = 0$ μm, $y = 30$ μm). The flux densities in the top ($z = 17.1$ μm) and bottom ($z = 13.0$ μm) surfaces of upper yoke are larger than that in the middle part ($z = 15.0$ μm) due to the remarkable skin effect. B_ys at $z = 17.1$ μm and 13.0 μm are more sensitive to the applied *mmf* waveform than the head field and B_y at 15.0 μm. They are firstly increased, then decreased.

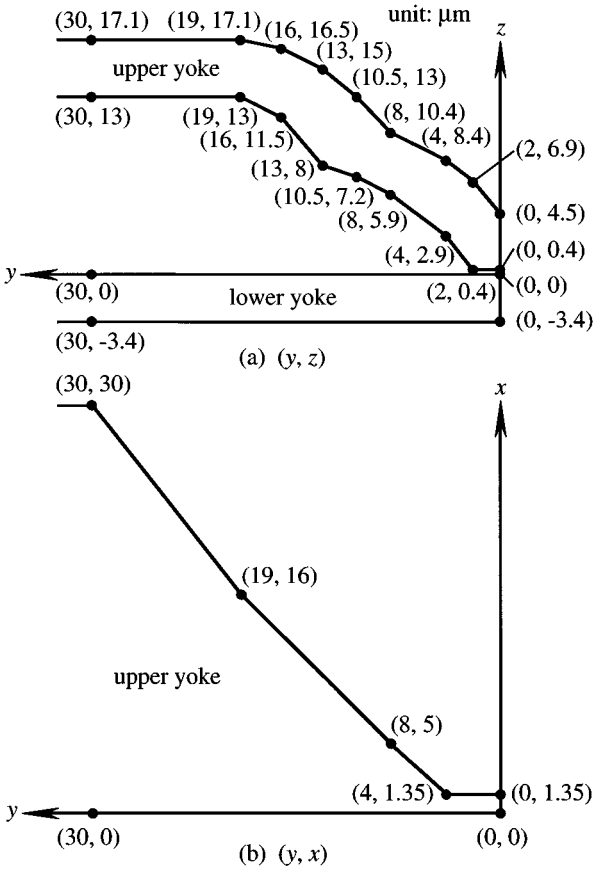

Fig. 5. Detailed dimensions of pole tip.

On the contrary, B_y at 15.0 μm increases gradually with time. Although the deviation of B_y is slightly larger than that of head field shown in Fig. 3, the deviation may be acceptable with the exception of no. 4 and some parts around 15 ns of no. 3.4.

V. Conclusion

It is shown that the eddy current analysis of thin film write head is possible by using the edge-based finite element method. The difficulty of generating mesh and the extent of number of elements and CPU time for such a write head, having very narrow gap and pole tip of 1 μm order, are clarified.

The result of this paper using the benchmark problem will give useful suggestions for analyzing a thin film write head for higher magnetic recording density, such as 100 Gb/in^2. The development of combined method of ordinary macroscopic analysis and micromagnetics theory is the future work for the optimal design of high density write head using numerical analysis.

Appendix

Fig. 5 shows the detailed dimensions of pole tip. Table II is the typewritten data of the applied magnetomotive force.

TABLE II
Applied Magnetomotive Force

time (ns)	*mmf* (A• turns)	time (ns)	*mmf* (A• turns)	time (ns)	*mmf* (A•turns)
6.5	-0.43088	18.0	0.46444	30.0	-0.39338
7.0	-0.41681	18.5	0.47850	30.5	-0.50588
7.5	-0.30431	19.5	0.45975	31.0	-0.51056
8.0	-0.05588	20.0	0.45975	31.5	-0.49181
8.5	0.17850	20.5	0.45975	32.0	-0.46369
9.0	0.31444	21.0	0.46913	32.5	-0.44963
9.5	0.38006	21.5	0.46444	33.0	-0.43088
10.0	0.37538	22.0	0.46444	33.5	-0.42150
10.5	0.34725	22.5	0.45506	34.0	-0.41213
11.0	0.37538	23.0	0.46444	34.5	-0.40744
11.5	0.44569	23.5	0.46444	35.0	-0.40275
12.0	0.49256	24.0	0.46444	35.5	-0.41681
12.5	0.48788	24.5	0.45975	36.0	-0.43088
13.0	0.45506	25.0	0.45975	36.5	-0.43088
13.5	0.42225	25.5	0.45975	37.0	-0.43088
14.0	0.42694	26.0	0.45506	37.5	-0.43556
14.5	0.43631	26.5	0.45038	38.0	-0.43088
15.0	0.45975	27.0	0.41756	38.5	-0.43088
15.5	0.45975	27.5	0.31444	39.0	-0.44494
16.0	0.45975	28.0	0.13163	39.5	-0.43088
16.5	0.45506	28.5	-0.00900	40.0	-0.44025
17.0	0.45975	29.0	-0.11681		
17.5	0.45975	29.5	-0.23869		

Acknowledgment

The authors would like to acknowledge K. Hayashi, T. Miyauchi and K. Kitamura for their organization of this work.

References

[1] Y. Kanai, "Analysis of magnetic recording write heads—Magnetic recording simulations in Japan," *ICS Newsletter*, vol. 6, no. 1, p. 8, November 1998.

[2] A. Kameari, "Three dimensional eddy current calculation using edge elements for magnetic vector potential," in *Applied Electromagnetics in Materials*, K. Miya, Ed: Pergamon Press, 1989, pp. 225–236.

[3] K. Fujiwara, T. Nakata, and H. Ohashi, "Improvement of convergence characteristic of ICCG method for the $\boldsymbol{A} - \phi$ method using edge elements," *IEEE Trans. Magn.*, vol. 32, no. 3, pp. 804–807, May 1996.

[4] S. Niikura and A. Kameari, "Analysis of eddy current and force in conductors with motion," *IEEE Trans. Magn.*, vol. 28, no. 2, pp. 1450–1453, March 1992.

[5] H. Shinada, H. Suzuki, S. Sasaki, H. Todokoro, H. Takano, and K. Shiiki, "Time-resolved measurement of micro-magnetic field by stroboscopic electron beam tomography," *IEEE Trans. Magn.*, vol. 28, no. 5, pp. 3117–3122, September 1992.

[6] T. A. Manteuffel, "An incomplete factorization technique for positive definite linear systems," *Math. Comp.*, vol. 34, no. 150, pp. 473–497, April 1980.

[7] K. Fujiwara, T. Nakata, and H. Fusayasu, "Acceleration of convergence characteristic of the ICCG method," *IEEE Trans. Magn.*, vol. 29, no. 2, pp. 1958–1961, March 1993.

[8] A. Kameari, "Convergence of ICCG method in FEM using edge elements without gauge condition," *IEEE Trans. Magn.*, vol. 33, no. 2, pp. 1223–1226, March 1997.

[9] W. J. Schroeder and M. S. Shephard, "A combined octree/Delaunay method for fully automatic 3-D mesh generation," *Int. J. Numer. Methods Eng.*, vol. 29, no. 1, pp. 37–55, January 1990.